

High accuracy proper motions in crowded fields

C. Alard

¹ Institut d'Astrophysique de Paris, 98bis boulevard Arago, 75014 Paris France, e-mail: alard@iap.fr

² Observatoire de Paris, 77 avenue Denfert Rochereau, 75014 Paris France.

Abstract. The image subtraction method is a powerful tool to analyze the light variations in crowded fields. This method is able to achieve a nearly optimal differential photometry, even in very dense regions. However, image subtraction is not limited to photometry, and it is shown in this paper that the method can be generalized to the measurement of the differential proper motions. It is important to emphasize that image subtraction can reconstruct an un-biased frame to frame astrometric transform. A nearly optimal determination of this astrometric transform can be performed by expanding the spatial variations of the kernel using the derivatives of the constant kernel solution. It is demonstrated that an expansion using first and second derivatives is optimal. Differential refraction can be corrected easily using an artificial image and the first derivatives of the kernel. To illustrate the ability of the method to measure proper motions, a small sub-area near the center of a Galactic Bulge field covered 265 times by the OGLE II experiment has been selected. The resulting astrometric accuracy is very close to the photon noise for the faint objects, while for the brighter ones it approaches closely the limit set by the residual seeing fluctuations on the smaller scales. The accuracy obtained with this new method is compared to the accuracy achieved using classical methods. The improvement obtained varies from a factor of $\simeq 2$ for the brighter objects, to more than a factor of 3 for the fainter ones. This improvement is typical of the improvement that was obtained for the measurement of the photometric variations.

Key words. Techniques: image processing, Astrometry, Stellar dynamics

1. Introduction

The development of the image subtraction method was motivated by the need to perform an optimal analysis of the light variations in crowded stellar fields. In particular, the large amount of data produced by the microlensing surveys towards the Galactic Bulge or the LMC (Udalski *et al.* 1994 (OGLE), 1997 (OGLE II), Alcock *et al.* 1997 MACHO, Alard & Guibert 1997 (DUO)) posed the problem of the optimal detection and measurements of the light variations of a faint object surrounded by a dense background of stars. The first successful attempts were performed by Tomaney & Crotts (1996) who developed a Fourier based image subtraction method. This work was followed by a least-square implementation of the image subtraction method Alard & Lupton (1998). This least-square implementation is nearly optimal provided that the kernel solution is almost constant across the image. However this is not always the case, and sometimes it can be a severe limitation. As a consequence the least-square method was generalized to the case of spatially variable kernel solution with conservation of flux (Alard 2000). The ability of the least-square method to obtain nearly optimal results was demonstrated at many occasions (see for instance Alard 1999, or Wozniak 2002). It was also demonstrated that this method improved the photometry by a factor 2 to a factor 4, with respect to classical methods (see Alard 1999 for details). It was recently suggested by Paczyński (2002), that it might be possible to extend this improvement to the measurement of the stellar differential motions. As shown by Eyer & Wozniak (2001) it is possible to detect and estimate the proper motions of stars using the version of image subtraction optimized for photometric measurements. However, it is clear that to perform a nearly optimal astrometric measurement, it necessary to extend and develop substantially the image subtraction method.

2. Basic equations

An observed image is the result of the application of several physical process to the “true image”. The three major process are instrumental and atmospheric blurring, the sampling introduced by the detector array, and the noise. Each

of these process can be described appropriately by simple mathematical operations. It is of particular importance to image subtraction that the instrumental and atmospheric blurring of the image can be described appropriately by a convolution process. As a result it should be possible to transform an image to exactly the same observing condition as another one by a convolution process. The basic idea of image subtraction is that this convolution kernel can be written as sum of linear functions. Considering that the kernel ϕ takes the values $\phi_{i,j}$ on the image 2 dimensional grid, and that the basis functions f^k takes the corresponding values f_{ij}^k on the same grid, one can write:

$$\phi_{ij} = a_{ij} f_{ij}^k$$

in order to simplify the notation, the summation symbol will be omitted. The following implicit summation rule will be used: **summation occurs when the index is repeated twice.**

In general the coefficient a_j of the kernel decomposition will depend upon the position in the image, thus:

$$\phi_{ij} = a_j(x, y) f_{ij}^k \quad (1)$$

By applying this kernel transform to the best seeing image G , it is possible to match closely the other image. Assuming Gaussian statistics the optimal kernel transform should minimize the chi-square between the convolved image and the bad seeing image B .

$$\chi^2 = \left\| \frac{a_k G_{i-l, j-m} f_{lm}^k - B_{ij}}{\sigma_{ij}} \right\|^2$$

To simplify the notations it is interesting to define the convolved basis functions:

$$W_{ij}^k = G_{i-l, j-m} f_{lm}^k$$

Thus:

$$\chi^2 = \left\| \frac{a_k W_{ij}^k - B_{ij}}{\sigma_{ij}} \right\|^2 \quad (2)$$

3. Image subtraction and optimal astrometry

3.1. modeling of differential motions

To perform optimal astrometry one has to measure the displacements of stars between 2 images with the best possible accuracy. The displacements due to proper motions of stars corresponds to tiny shifts on the image grid. It is possible to model such small shifts in a given image I with great accuracy using a first order expansion in spatial coordinates:

$$\delta I_{ij} = \left(\frac{\partial I}{\partial x} \right)_{ij} dx + \left(\frac{\partial I}{\partial y} \right)_{ij} dy \quad (3)$$

Thus to model the displacements between our 2 images it is necessary to introduce the local derivatives. Our model of the image is (see eq 2):

$$M_{ij} = a_k W_{ij}^k$$

According to eq (3) the shifted model \tilde{M} can be written:

$$\tilde{M}_{ij} = M_{ij} + \left(\frac{\partial M}{\partial x} \right)_{ij} dx + \left(\frac{\partial M}{\partial y} \right)_{ij} dy$$

Note that:

$$\left(\frac{\partial M}{\partial x} \right)_{ij} = \frac{\partial}{\partial x} (B_{i-l, j-m} \phi_{lm}) \simeq \frac{\partial}{\partial x} \int B(u, v) \phi(x-u, y-v) dudv \simeq \int B(u, v) \frac{\partial}{\partial x} \phi(x-u, y-v) dudv$$

Consequently:

$$\left(\frac{\partial M}{\partial x} \right)_{ij} \simeq B_{i-l, j-m} \left(\frac{\partial \phi}{\partial x} \right)_{lm}$$

Thus, we see that it is possible to model small shifts between the image by including the derivatives of the kernel in the kernel expansion. Provided that the kernel basis is complete this basis should also contain the kernel derivatives (as a linear combination of the original basis function). As a consequence it is clear that the general image subtraction method should be able to model small shifts between the images. Since the kernel decomposition depends on the position in the image, the shift may also depend on the position. However, we may wonder if this mapping of the shifts between the images corresponds to the right astrometric registration.

3.2. Image subtraction and astrometric alignment

One condition for the perfect astrometric alignment between 2 systems is that there should be no systematic offset between the 2 systems. Thus it is important to check that the subtracted image does not contains some systematics astrometric shift. A residual shift in the subtracted image would mean that there is a displacement between the convolved solution and the image to fit. Assuming that the unshifted subtracted image is R_{ij} , and that the bad seeing image B_{ij} is shifted by (δ_x, δ_y) with respect to the convolved good seeing image $a_k W_{ij}^k$, using eq (3) one can write that the shifted subtracted S_{ij} image will be:

$$S_{ij} = a_k W_{ij}^k - B_{ij} = R_{ij} + \left(\frac{\partial B}{\partial x} \right)_{ij} \delta x + \left(\frac{\partial B}{\partial y} \right)_{ij} \delta y$$

Thus the estimation of the displacement is once again a linear least-squares problem related to the estimation of (δ_x, δ_y) . Here the 2 least-squares vectors are the derivatives of the image. The corresponding normal least square equation is a linear system of equations with the following form:

$$N \delta_{xy} = V \quad (4)$$

Where N is a matrix containing the cross products of the vectors. V is a vector which components are the cross products of the vectors with the subtracted image. For the ideal, unshifted solution, R_{ij} , $\delta_{xy} = 0$, and consequently, according to eq (4), the cross products:

$$\frac{R_{ij}}{\sigma_{ij}^2} \left(\frac{\partial B}{\partial x} \right)_{ij} \quad \text{and} \quad \frac{R_{ij}}{\sigma_{ij}^2} \left(\frac{\partial B}{\partial y} \right)_{ij}$$

have to be zero. It is possible to demonstrate the same result for the shifted subtracted image. The image subtraction method implies that χ^2 must be minimal with respect to any the kernel coefficient a_p , using eq (2) one can write:

$$\frac{\partial \chi^2}{\partial a_p} = 0 = W_{ij}^p \left[\frac{a_k W_{ij}^k - B_{ij}}{\sigma_{ij}} \right] = W_{ij}^p R_{ij} \quad (5)$$

As it was already shown in Sec. 3.1 the kernel basis of functions should contain the kernel derivatives. A convolution with the kernel derivatives will recreate the derivatives of the image. Thus the basis of functions W_{ij}^p should contain the image derivatives. Then using eq (5) it is easy to prove that the scalar product of the image derivatives with the subtracted image is zero. And consequently using eq (4), we see that the displacement δ_{xy} has to be zero. Thus there is no systematic bias on in an astrometric registration performed using the image subtraction method.

4. Optimal astrometric alignment

The general image subtraction method is able to perform an unbiased image alignment, however the least-square process, and in particular the spatial variability involves a large number of free parameters which may introduce unnecessary noise. To perform an optimal astrometric alignment it is required to use the smallest possible set of parameters. Image subtraction with spatial variations requires many parameters. To estimate the number of parameters, it is necessary to multiply the numbers of parameters for the constant kernel solution by the number of polynomial coefficients used the spatial expansion. Typically, a constant kernel solution requires about 50 parameters and with a spatial expansion of second degree we get 300 parameters. However, if we consider a smaller region of the image, we expect that the spatial variation of the kernel will be small, and that we might be able to model the kernel variations using an expansion in Taylor series of the constant kernel solution ϕ^0 (ϕ^0 can be for instance the solution near the center of the frame):

$$\phi_{ij} = \phi_{ij}^0 + \sum_{l <= k} a_{kl}(x, y) \left[\frac{\partial^{k+l} \phi^0}{\partial x_k \partial y_l} \right]_{ij} \quad (6)$$

It is particularly interesting to use a Taylor series of degree 2. In this expansion, the first derivatives will take into account the motion between the frames, while the second derivatives will help to reduce the general chi-square. It is important to note that the components corresponding to the astrometric displacement $(\frac{\partial \phi^0}{\partial x}, \frac{\partial \phi^0}{\partial y})$ are orthogonal to the other components of the kernel expansion. For instance:

$$\int_{-\infty}^{\infty} \frac{\partial \phi^0}{\partial x} \phi^0 dx = \left[\frac{1}{2} (\phi^0)^2 \right]_{-\infty}^{\infty} = 0 \quad (\text{Since the kernel decreases exponentially})$$

Similarly, one can demonstrate easily that the first derivatives are orthogonal to the second derivatives. This property is also true for the convolved basis functions. The convolution with the kernel derivatives will give the derivatives of the convolved image. Thus, our former reasoning will apply. Except, that here the relevant integration boundaries will be the edges of the image. The image may not be zero on its edges, but what matter for the value of the integral is the difference between the edges. Statistically if the value on the edges are un-correlated, the mean should be zero. In any case the cross-product of the first derivative with the 2 others component should be very small. Thus, the least-squares vectors corresponding to the kernel derivatives are orthogonal to the other least-square vectors. In the least-square normal equations, the matrix contains the cross products of the vectors, and thus many components of the matrix will be zero. This matrix will be non-zero only in local blocks. In particular, the block corresponding to the first derivatives will be isolated, and surrounded with zeros. As a result the least-square solution for the first derivatives will be independent from the estimation of the other parameters. This property is very interesting, because it means that the errors will be also independent on the errors on the other parameters, and as a consequence should be minimized. Note that formally the scalar product of the vectors, represent the least-square matrix element in case the statistically weight σ_{ij} is constant (gaussian noise). In case of Poissonian weighting, the difference should be negligible in most area, except for bright stars. But even around bright stars, provided the psf is nearly symmetrical, one can show that in this case the integral is close to zero. Thus it means that the errors on estimation of the astrometric displacement will be minimal. This interesting property of the spatial dependence in terms of derivatives could be completely flawed if the spatial expansion did not conserved the flux. Hopefully it is easy to demonstrate that the derivatives have zero sums. For instance:

$$\int_{-\infty}^{\infty} \frac{\partial \phi}{\partial x} dx = [\phi]_{-\infty}^{\infty} = 0 \quad \text{Since the kernel decreases exponentially}$$

The same reasoning apply to all the other derivatives. Thus, using eq (5) we see immediately that the integral of the kernel as a function of position is constant, and is equal to the integral of the constant kernel solution. As a conclusion, we see that the Taylor expansion of order 2 provides a natural basis to expand the spatial variations of the kernel: the errors on the differential motions are minimized, and flux conservation is preserved.

5. Correction of differential refraction

To first order, the effect of differential refraction is to shift slightly the position of the stars. The amplitude of the shift depends on the color of the stars. Thus to correct the differential refraction, one must know the color of the objects in the image. To compute the color of the objects it is necessary to run a source extraction code in the V and I band. The magnitudes in each band are estimated by PSF fitting. Once the color and magnitude of each star are known, it is possible to correct for the differential refraction effect. For instance assuming a simple model where the displacement is proportional to the color, the correction will be proportional to the color of the star multiplied by its flux. In this simple model, to compute the differential refraction correction it is sufficient to reconstruct an artificial image where the amplitude of the stars are multiplied by their color, and convolve it with the kernel derivatives. A least-square fit of these 2 vectors will give directly the 2 coefficients corresponding to the differential refraction along x and y. Obviously the method can be extended to non-linear modeling of the color versus differential refraction effect.

6. Application to OGLE data

6.1. practical implementation

The OGLE II project (Udalski *et al* 1997) produced a large amount of good quality CCD image in either Galactic or Magellanic fields. Most of the data is in the I band, with also some images in V and B. Some of the Galactic Bulge fields offers an impressive coverage of the observing seasons. In particular the field OGLE Bulge SC 33 has been observed 265 times over an interval of approximately 1200 days. This data set is very well suited to experiment the new method presented in this paper. In this field the density of stars is very large, and thus it is sufficient to study a smaller sub-area of the field. The area selected is near the center of the SC 33 field, the Galactic coordinates of the center of the field are: (l=2.2, b=-3.7). An image surface of 512×512 pixels which corresponds to about 3.5' × 3.5' on the sky is large enough to give a total of about 800 stars for which the color and magnitudes can be measured with decent accuracy. Although it is important to note that due to the severe blending, this may not be true for the fainter objects, which actually can be unresolved blends. Due to this source confusion issue, it is interesting to have the best possible spatial resolution in the reference image. One of the image was taken under outstanding seeing conditions, with low airmass. This image has also the advantage to be near the middle of the data time interval, which minimize the differential motion of the stars. All the frame were aligned to this reference frame (see Alard & Lupton 1998, and Alard 2000 for details), and then subtracted. The constant kernel solution was derived by a local fit on the bright stars. The solution that was selected is the local solution having the best χ^2 for the whole image. The

derivatives of the constant kernel solution were expanded spatially using polynomials of 2nd degree. The differential refraction was corrected using a polynomial of the same degree. Thus, the total number of components to fit on the image using linear least-square is 43. In order to minimize the errors due to the drift scan procedure, the frame was splitted into 3 sub-frames along the y direction . Using the full set of 265 subtracted images, it is possible to produce astrometric curves along each direction for the 782 stars of the sample. Knowing the baseline flux of the star F_0 , the local kernel solution ϕ , and the local psf on the reference image, ψ , one can relate the displacement to the residuals in the subtracted image S_{ij} using eq (3):

$$S_{ij} = F_0 \left(\frac{\partial \eta}{\partial x} \right)_{ij} dx + F_0 \left(\frac{\partial \eta}{\partial y} \right)_{ij} dy \quad \text{with :} \quad \eta_{ij} = \phi_{i-j,k-l} \psi_{k,l}$$

Thus dx and dy can be measured by a 2 parameter linear least-square fit:

$$S_{ij} = a_0 \left(\frac{\partial \eta}{\partial x} \right)_{ij} + a_1 \left(\frac{\partial \eta}{\partial y} \right)_{ij} \quad \text{with :} \quad dx = \frac{a_0}{F_0}, \quad dy = \frac{a_1}{F_0} \quad (7)$$

The differential motions of each star in each of the 265 frames was estimated using eq (6). To estimate the proper motion of the star, the curve representing its displacement as a function of time was fitted with a straight line. This fit gives also the opportunity to compute the error on the estimation of the slope (proper motion). The brightness of the star F_0 was derived by PSF fitting (see also Sec. 5).

6.2. The errors on the proper motion

In principle the error on the slope should be derived directly from the Poisson fluctuations. However, the real errors exceeds the Poisson expectations, and especially for bright stars (see Fig. 1). Obviously, there are other causes of uncertainties that are larger than the Poisson fluctuations for bright stars. These cause do certainly include the seeing fluctuations, and possibly also, the variation of sensitivity on the surface of a pixel, the noise in the flat fielding, and finally the drift . It is simple to analyze each of these causes separately. First the seeing fluctuations: in Alard & Lupton (1998) it was shown that on a scale of an arc minute the variation of the centroid position due to the seeing fluctuations was about 10 mas. However, since in the present work it is possible to correct the systematic spatial variations between the 2 images to subtract, at least, the large scale seeing fluctuations should be corrected. Although, it is clear that nothing can be done on smaller scales: typically a few arc seconds. To be more specific the seeing fluctuations cannot be corrected on a distance smaller than the minimum separation between 2 resolved stars, which is about 10 pixels \simeq 4 arc seconds. Since the seeing fluctuations between 2 stars separated by θ decreases like $\theta^{1/3}$, and that there are 265 data points, a quick estimate of the error gives $\simeq (4/60)(1/3) * 10/\sqrt{265} \simeq 0.25$ mas. The other errors except possibly the uncertainties in the flat fielding are much smaller. Numerical simulation shows that the variations of sensitivity on the surface of a pixel should be at least one hundred time smaller than the errors due to the seeing fluctuations. In case the drift scan errors would contribute significantly to the error budget, we would see a different between the errors in each direction. But Fig. 1 shows that this is not the case. The last possibility to investigate are systematic flat fielding errors on the scale of the PSF. For a 1 arc second seeing, a systematic flat fielding variation (with the right shape) of 1 % would translate into a variation of 7 mas of the centroid, corresponding to a global error on the proper motion of about 0.4 mas. But it is important to emphasize, that it is unlikely to find systematic variation in the flats on the scale of the PSF, and that it is less likely again that these systematic variations have the right shape (the shape of the derivatives). As a conclusion it is very likely that most of the excess in the astrometric error for bright stars is due to residual seeing fluctuations on smaller scales.

6.3. Testing the accuracy of the method

The recent release by Sumi *et al.* (2003) of a large scale study of the proper motions of stars in a large number of OGLE Bulge fields offers the possibility to compare the accuracy achieved using this method to the accuracy obtained using classical methods (DoPHOT). By comparing Fig. 2 in this paper to Fig. 4 in Sumi *et al.* (2003), we can estimate that for clump giants ($I \simeq 15.5$) Sumi *et al.* obtain a mean accuracy slightly above 1 mas \simeq 1.2 mas, while Fig. 2 in this work gives an accuracy of \simeq 0.4 mas. This improvement of factor of 3 in the accuracy is also typical of the improvement obtained for the photometry. Note that the brighter unsaturated stars this improvement is closer to a factor of 2, while for the fainter stars it is a little above 3. One may wonder why such an improvement is observed even on the bright stars. The answer might be that in classical methods to perform an optimal measurement of the position of a star it is necessary to build a psf model for each new image. Image subtraction does not need a psf model. The measurement of the motions in the subtracted images, requires to build a psf model only for the reference image. There is no need to re-create a psf model for each new image. As the calculation of the position is quite sensitive to the psf

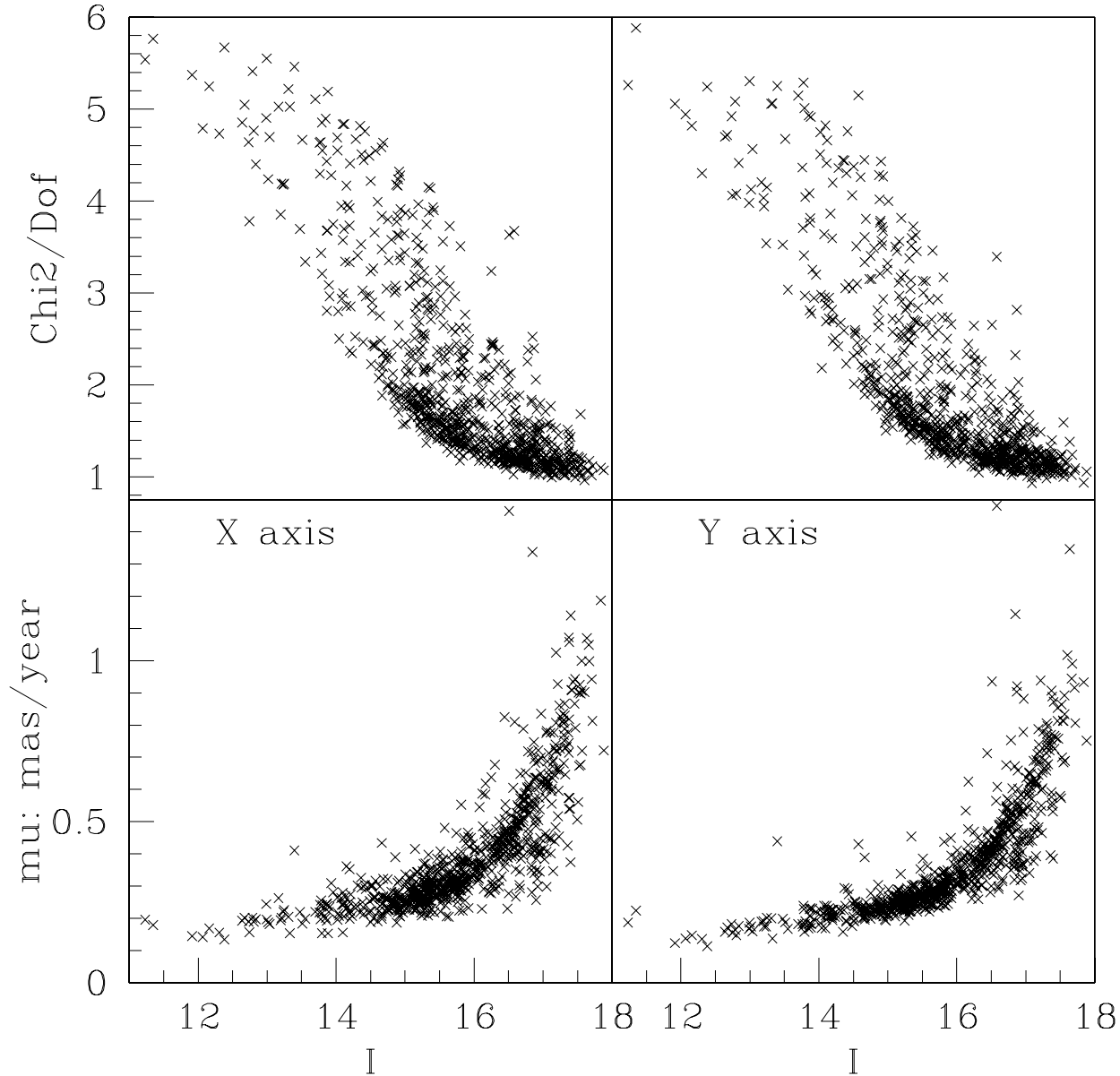


Fig. 1. The error on measuring the proper motion along the X and Y directions as a function of the I band magnitude for the 782 stars of the sample. The diagrams in the bottom presents the real value of the errors, while on the top the errors are compared to the theoretical poissonian expectations.

model, this result certainly in a reduction of the noise. As a final testing it is interesting to investigate the structure of the proper motions as a function of color and magnitudes. The proper motions along the Galactic longitude and latitude (l, b) have been represented in Fig. 3 as a function of color. The bluer stars belong to the disk population, and show a systematic motion along the l axis as expected from the differential rotation between the Galactic disk and bulge. No systematic motion are observed along the b axis. Fig. 3 includes all stars in the sample, whatever the accuracy achieved on these objects, there was no attempt to perform any cut-off in the error distribution. Since the disk stars have systematic positive motions in longitude, it should be possible to reject the disk stars and to retain only the bulge stars by selecting stars having negative motions in l . Stars having negative l motions have been selected by means of a 3σ cuts. Their position in the color-magnitude diagram is presented in Fig. 4. Two different cuts have been used. The first cut in the lower panel favors the maximum number of stars by allowing the fainter star to enter the selection. The second panel presents stars having accurately measured proper motions, thus allowing a lower cut-off, but also restricting the selection to the brighter objects. An interesting feature start to appear in the lower panel:

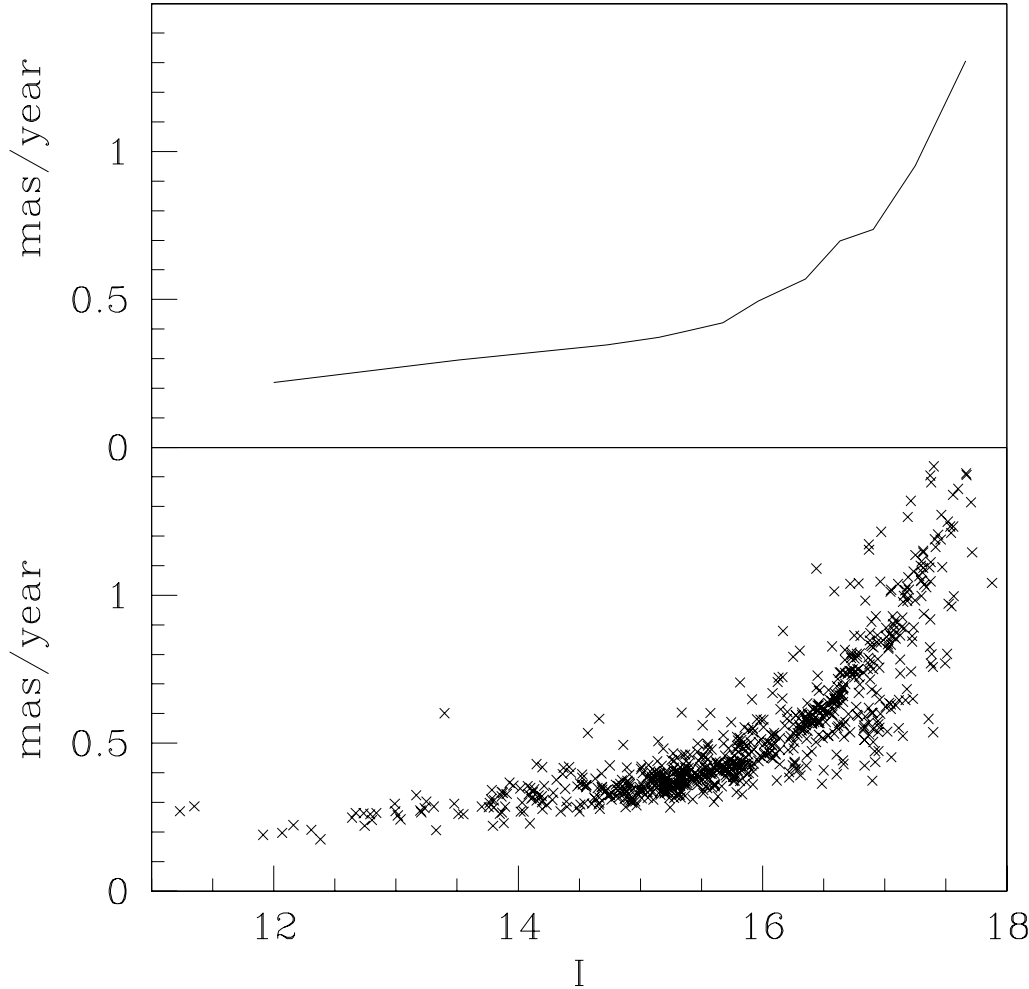


Fig. 2. The error on measuring the proper motion as a function of the I band magnitude for the 782 stars of the sample. Note that one star near the magnitude $I=13$ has a large deviation from the rest of the sample. Although this star is unsaturated, it is very close to a very bright saturated star. The diagram at the bottom presents the errors for each stars, while the diagram on the top gives the mean error.

there are a few stars just above the main sequence. Even if the kinematics of these stars overlaps the Bulge kinematics these stars are probably not Bulge stars. The upper panels reveals their true nature: we see a well defined sequence, just parallel to the main sequence but just a little above. These stars are most likely wide binaries. These binaries belongs to the disk population, but the long period motion of their center of gravity alter their proper-motions, to the point that they overlap some of the Bulge kinematics. The ability of the method to find these stars indicates that the method is really accurate. In the lower panel of Fig. 4 there are also some stars below the main sequence. These stars could be white dwarfs. A further examination of a larger sample will help to confirm this possibility. As a final test of these proper motions, it is interesting to compare the velocity dispersion of the Bulge stars to the recent results obtained by Kuijken & Jones (2002). Most of the clump giants in this field belong to the Bulge population. Thus this is a good set of stars to estimate the Bulge velocity dispersion. By selecting stars in a small window around the clump it is possible to derive the following (l,b) proper motion dispersions: (2.76, 2.16) mas. Kuijken & Jones (2002) found (2.9, 2.5) mas for a field located close to OGLE SC 33. It is difficult to determine whether the smaller dispersion found in this study is related to the accuracy of the measurement of the proper motions, or is due to a different sampling of the Bulge stellar population. Assuming a distance to the Bulge of 8 Kpc, the proper motion dispersions measured in this study translate to respectively (105, 82) km/s. This result is consistent with the former study of Spaenhauer, Jones & Whitford (1992).

Acknowledgements. The author would like to thank B. Paczyński for interesting discussions and suggestions. The stay of the author in Princeton was supported by the NSF grant AST-1206213, and the NASA grant NAG5-12212 and funds for proposal

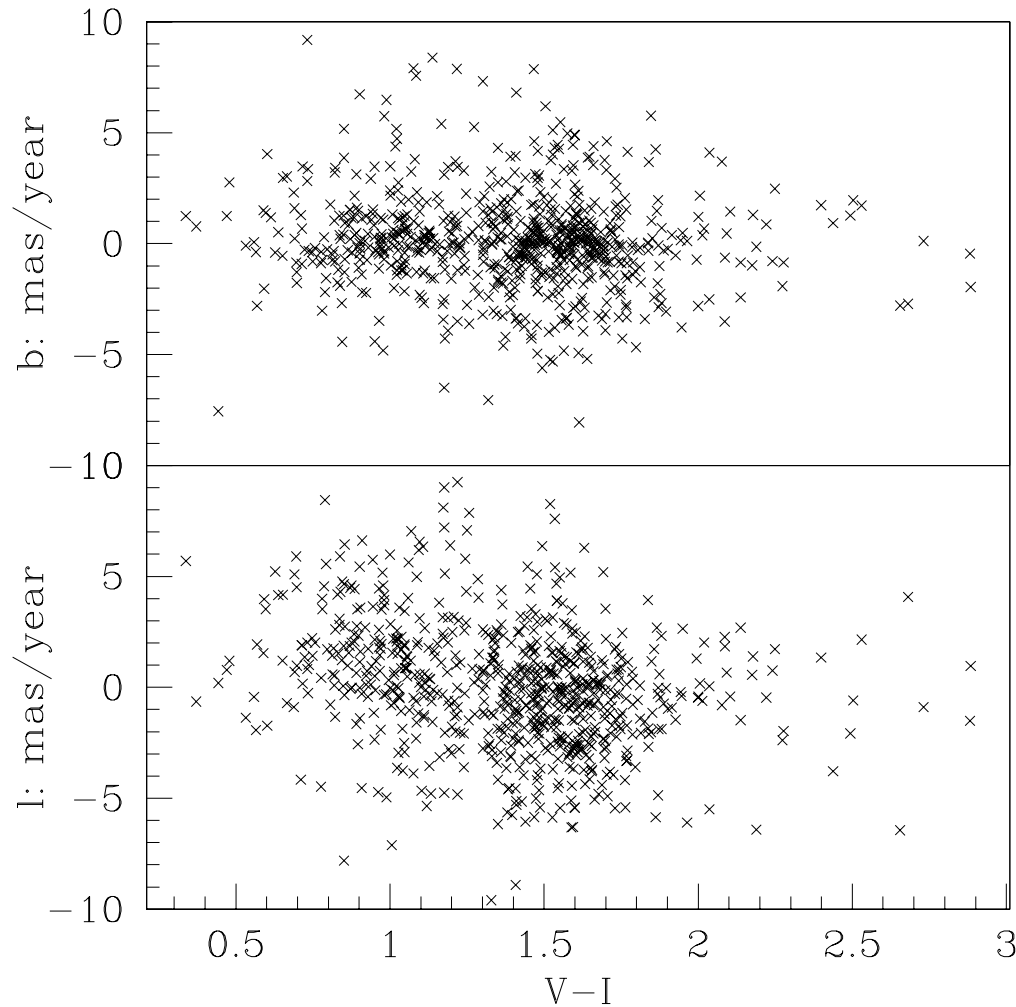


Fig. 3. The proper motion of the of all the stars in the sample along the (l,b) axis as a function of color. Note that the proper motions of the bluer stars are systematically shifted along the l axis, but not along the b axis.

#09518 provided by NASA through a grant from the Space Telescope Science Institute, which is operated by the Association of Universities for Research in Astronomy, Inc., under NASA contract NAS5-26555.

References

- Alard, C., 2000, *A&AS*, **144**, 363
 Alard, C., 1999, *A&A*, **343**, 10
 Alard, C., & Lupton, R., 1998, *ApJ*, **503**, 325
 Alard, C. & Guibert, J., 1997, *A&A*, **326**, 1
 Alcock, C., Allsman, R. A., Alves, D., Axelrod, T. S., Becker, A. C., Bennett, D. P., Cook, K. H., Freeman, K. C., Griest, K., Guern, J., Lehner, M. J., Marshall, S. L., Peterson, B. A., Pratt, M. R., Quinn, P. J., Rodgers, A. W., Stubbs, C. W., Sutherland, W., Welch, D. L., 1997, *ApJ*, **486**, 697
 Eyer, L., Wozniak, P., 2001, *MNRAS*, **327**, 601
 Kuijken, K., Rich, R., 2002, *AJ*, **124**, 2054
 Paczyński, B., 2002, Private communication.
 Spaenhauer, A., Jones, B., Whitford, A., 1992, *AJ*, **103**, 297
 Sumi, T., Wu, X., Udalski, A., Szymanski, M., Kubiak, M., Pietrzynski, G., Soszynski, I., Wozniak, P., Zebrun, K., Szweczyk, O., Wyrzykowski, L., 2003, astro-ph/0210381, submitted to *MNRAS*
 Tomaney, A., Crotts, A., 1996, *AJ*, **112**, 2872
 Udalski, A., Kubiak, M., Szymanski, M., 1997, *AcA*, **47**, 319
 Udalski, A., Szymanski, M., Stanek, K. Z., Kaluzny, J., Kubiak, M., Mateo, M., Krzeminski, W., Paczynski, B., Venkat, R., 1994, *AcA*, **44**, 165

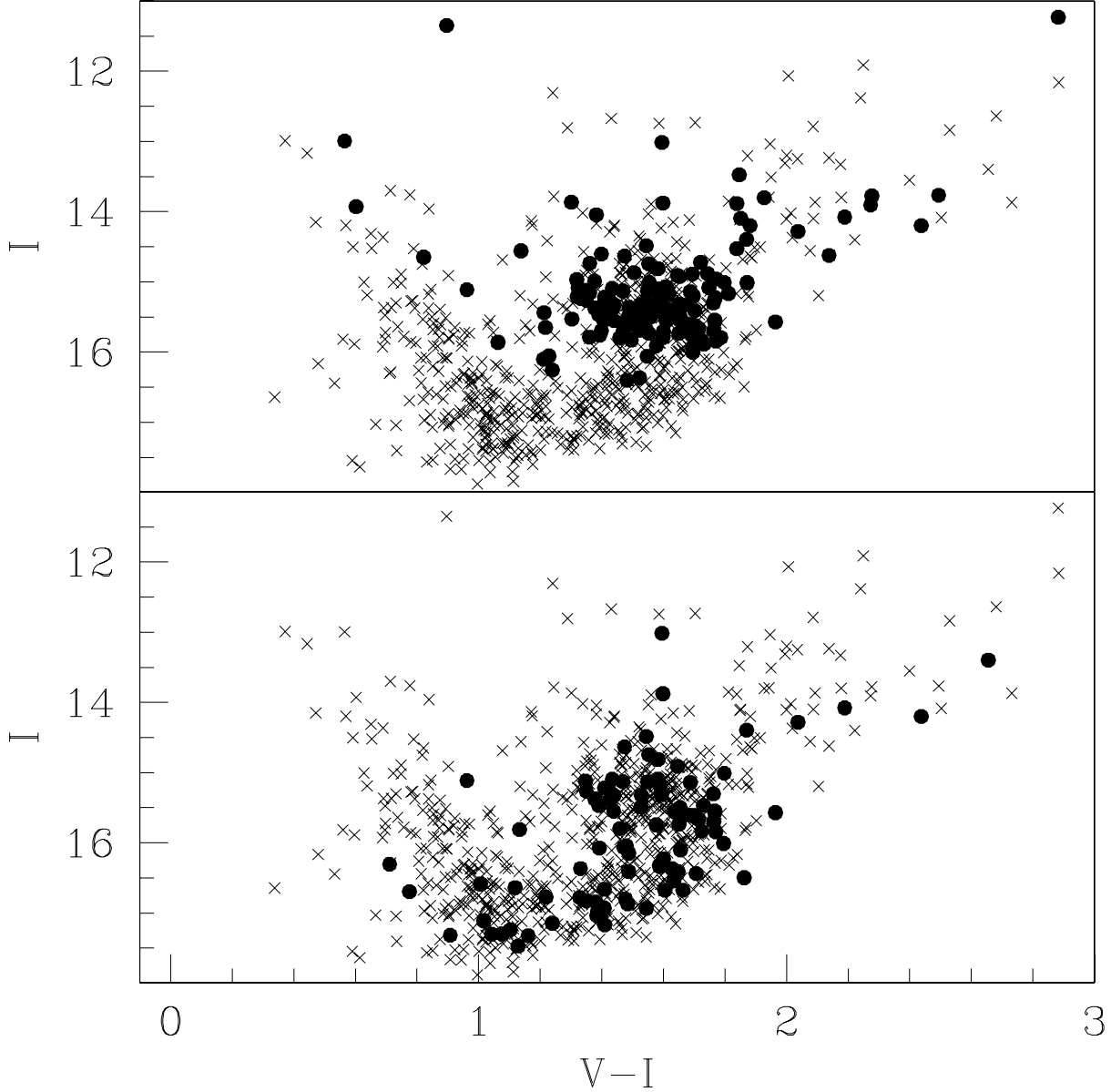


Fig. 4. Selection of stars having negative proper motions along the l direction. These stars should belong to the Bulge population. The cross represents all the stars while the bold dots represents negative l motion. Two different cuts have been performed: $\mu_l < -1$ plus error on $\mu < 0.35 \simeq 3\sigma$ below 0 (top), and $\mu_l < -2.5$ plus error on $\mu < 0.83$ (bottom). In the lower diagram, the Bulge sequence is well outlined. The top of the Bulge main sequence, as well as the Bulge sub-giants and giants are clearly visible. There also some stars below and above the main sequence. The the star below the main sequence could be white dwarfs. The star above the main sequence appear more clearly in the upper diagram (lower cut-off, better accuracy). These stars could be wide binaries.